

## Influence of Shoulder Abduction and Lateral Trunk Tilt on Peak Elbow Varus Torque for College Baseball Pitchers During Simulated Pitching

Tomoyuki Matsuo<sup>1</sup>, Glenn S. Fleisig<sup>2</sup>, Naiquan Zheng<sup>3</sup>, and James R. Andrews<sup>2</sup>

<sup>1</sup>Osaka University; <sup>2</sup>American Sports Medicine Institute; <sup>3</sup>University of Florida

Elbow varus torque is a primary factor in the risk of elbow injury during pitching. To examine the effects of shoulder abduction and lateral trunk tilt angles on elbow varus torque, we conducted simulation and regression analyses on 33 college baseball pitchers. Motion data were used for computer simulations in which two angles—shoulder abduction and lateral trunk tilt—were systematically altered. Forty-two simulated motions were generated for each pitcher, and the peak elbow varus torque for each simulated motion was calculated. A two-way analysis of variance was performed to analyze the effects of shoulder abduction and trunk tilt on elbow varus torque. Regression analyses of a simple regression model, second-order regression model, and multiple regression model were also performed. Although regression analyses did not show any significant relationship, computer simulation indicated that the peak elbow varus torque was affected by both angles, and the interaction of those angles was also significant. As trunk tilt to the contralateral side increased, the shoulder abduction angle producing the minimum peak elbow varus torque decreased. It is suggested that shoulder abduction and lateral trunk tilt may be only two of several determinants of peak elbow varus torque.

**Key Words:** forward kinematics, regression analysis, minimum torque

Elbow injuries due to throwing have been frequently reported and often require surgery on both youth and adult players (Andrews & Timmerman, 1995; Klingele & Kocher, 2002; Petty, Andrews, Fleisig, & Cain, 2004). The main cause of such pain during pitching is the valgus/varus torque (Sabick, Torry, Lawton, & Hawkins, 2004; Werner, Murray, Hawkins, & Thomas, 2002). At the approximate instant of maximum external rotation of the throwing shoulder, the elbow varus torque reaches a peak (Fleisig, Andrews, Dillman, & Escamilla, 1995). To resist the valgus torque generated during the arm cocking phase, tensile force almost equal to the maximum capacity of the ulnar collateral ligament is required (Fleisig et al., 1995).

In a study by Werner et al. (2002) using data from 40 professional baseball pitchers and multiple regression analyses, the varus torque during pitching correlated with four kinematic and kinetic variables. The significant variables among the 37 biomechanical variables tested were shoulder abduction angle at the instant of lead foot contact, peak angular velocity of shoulder horizontal adduction, elbow angle at the instant of peak varus torque, and maximum torque of shoulder internal rotation. Shoulder abduction angle was positively correlated to elbow varus torque. However, this finding did not agree with anecdotal information indicating that lower shoulder abduction is related

<sup>1</sup>Graduate School of Medicine, Osaka University, 1-17 Machikaneyama, Toyonaka, Osaka 560-0043, Japan; <sup>2</sup>American Sports Medicine Institute, 1313 13th St. South, Birmingham, AL 35205; <sup>3</sup>Dept. of Orthopaedics and Rehabilitation, University of Florida, Gainesville, FL 32601.

to an increased risk of elbow injury (House, 1990; Nobuhara, 2003; Norwood, Del-Pizzo, Jobe, & Kerlan, 1978). Further knowledge about the relationship between the elbow varus torque and shoulder abduction angle is needed.

It has also been reported that sidearm pitchers have a higher incidence of elbow injury and more severe symptoms than overhand and three-quarter-hand pitchers (Albright, Jokl, Shaw, & Albright, 1978). The main kinematic difference between these types of delivery is the lateral trunk tilt (Matsuo, Takada, Matsumoto, & Saito, 2000). Lateral trunk tilt seems to influence elbow varus torque. In addition, underhand pitchers (i.e., pitchers with ipsilateral trunk tilt) showed lower shoulder abduction angle, which highly correlated with the optimal shoulder abduction angle based on minimum square torque of the throwing arm (Matsuo, Matsumoto, Mochizuki, Takada, & Saito, 2002). Thus it was expected that lateral trunk tilt and its interaction with shoulder abduction angle affect elbow varus torque. However, we know of no published study investigating this relationship.

The purpose of the present study was to examine the effects of shoulder abduction angle and lateral trunk tilt on elbow varus torque, by means of computer simulations and regression analyses. Specific problems to be solved in this study were: (a) to confirm that there are shoulder abduction angles which minimize elbow varus torque or cause high elbow varus torque that should be avoided; (b) to determine whether shoulder abduction angles are influenced by lateral trunk tilt angles; (c) to investigate whether there are any individual differences in the pattern of change in peak elbow varus torque when shoulder abduction angle and lateral trunk tilt angle are changed; and (d) to compare the results from simulation analyses with those from regression analyses.

## Methods

Thirty-three healthy college baseball pitchers participated in the study. Of these, 24 were right-handed pitchers and 9 were left-handed pitchers. All of them were overhand and three-quarter-hand pitchers. Their mean age, height, and mass were  $20.1 \pm 1.1$  years,  $1.85 \pm 0.04$  m, and  $82.5 \pm 8.6$  kg, respectively. Mean ball velocity in the recording session described below was  $36.8 \pm 0.9$  m/s. After

the pitchers completed informed consent and history forms, their body weight, height, humerus length, and radius length were measured. Each participant was provided an unlimited amount of time for stretching and nonthrowing drills.

Reflective markers (38 mm diameter) were then attached bilaterally at the lateral malleoli, lateral femoral epicondyles, greater trochanters, lateral superior tip of the acromions, and lateral humeral epicondyles. A reflective marker was also attached at the ulnar styloid process of the nonthrowing wrist, while a reflective band (1 cm wide) was placed around the throwing wrist.

Motion data were collected using four 200-Hz infrared cameras (Motion Analysis Corp., Santa Rosa, CA) in an indoor laboratory after unlimited warm-up throwing. Each participant threw 5 to 8 fastball pitches toward a strike zone indicated by ribbon on a net over home plate at the regulation distance (18.4 m) from the pitching rubber, with approximately 30 to 60 seconds rest between pitches. Ball speed was measured using a radar gun (Jugs Pitching Machine Co., Tualatin, OR) from behind the home plate. Three-dimensional locations of the reflective passive markers and band were calculated with an automatic digitizing system (Motion Analysis Corp.) utilizing the direct linear transformation method (Abdel-Aziz & Karara, 1971). Missing frames were handled with a fill-gap procedure using cubic spline function built in the Motion Analysis software. After checking position and velocity curves qualitatively, we discarded any trial in which the data did not show smooth curves.

The root mean square error in the calculation of the 3D marker location, with a calibration matrix approximately  $1.5 \text{ m} \times 1.2 \text{ m} \times 1.2 \text{ m}$  in size, was found to be less than 10 mm. Coordinate data were filtered with a Butterworth digital low-pass filter. Qualitative evaluation of velocity and acceleration data, based on the residual analyses and previous studies (Fleisig et al., 1996; Zheng, Fleisig, Barrentine, & Andrews, 2004), indicated that filtering with a cutoff frequency of 13.4 Hz is effective at rejecting noise and passing data.

From the locations of surface markers, the centers of the throwing elbow and shoulder joint were estimated using the same methods used in earlier studies (Fleisig et al., 1996). First the locations of joint centers and surface markers were manually

digitized for a small sample of participants. Then the locations of the throwing elbow and shoulder joint centers were expressed as a function of the local reference frames using the surface markers and the length of a pitcher's humerus and radius (Fleisig et al., 1996).

A pelvis local coordinate ( $R_p$ ), a trunk local coordinate ( $R_t$ ), and an upper arm coordinate ( $R_u$ ) were then calculated for each participant (Appendix A). Shoulder abduction angle was defined as the angle between a unit vector of the longitudinal axis for the upper arm ( $Z_u$ ) and the inferior unit vector of the trunk ( $-Y_t$ ); that is, a posture in which the arm hung vertically down was  $0^\circ$ , and a posture in which the elbow was level with the shoulder was  $90^\circ$  of abduction. The lateral trunk tilt angle was defined as the angle between the vertical axis of the trunk ( $Y_t$ ) and the vertical axis of the pelvis coordinate ( $Y_p$ ) in the plane of  $Y_t$  and  $Z_t$  (see Figure A in Appendix). A negative trunk tilt indicated that the trunk was tilted to the throwing arm side (ipsilateral tilt), and a positive tilt indicated that the trunk was tilted to the nonthrowing arm side (contralateral tilt).

Based on the results of our pilot study showing the similarity of kinematic and kinetic variables across pitches within a participant, the fastest fast-ball thrown for a strike was chosen, and the motion data from 0.1 s before lead foot contact to 0.1 s after ball release were used in the following analyses.

Direct kinematics using a matrix transformation was employed to calculate the joint positions for the simulated motions. Variations from the actual pitching motion were simulated by means of rotating  $X_t$  and  $X_u$  axes, respectively. The simulated angles at the instant of ball release for lateral trunk tilt were  $-20, -10, 0, 10, 20, 30,$  and  $40^\circ$ , and those for shoulder abduction angle were  $70, 80, 90, 100, 110,$  and  $120^\circ$ . Therefore, 42 ( $7 \times 6$ ) motions were generated for each participant. Figure 1 illustrates examples of the simulated motions selected as extreme conditions. Although the shoulder abduction angle and lateral trunk tilt angle were changed, all angular velocities remained the same as during the actual motions in order to isolate the effects of these variables on elbow varus torque.

The forces and torques at the throwing shoulder and elbow were calculated for the actual motion and simulated motions, using inverse dynamic equations of the Newton-Euler method with the kinematic data and reported segment inertia parameters using the

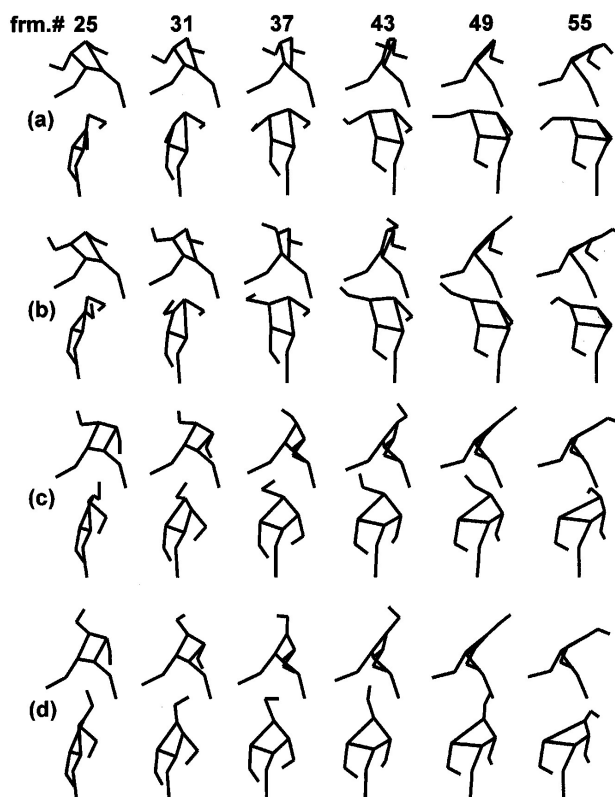


**Figure 1** – Side and front views of 4 extreme conditions among 42 simulated motions for one participant. (a) A simulated motion with ipsilateral trunk tilt (LTT =  $-20^\circ$ ) and low shoulder abduction (SA =  $70^\circ$ ) at the instant of ball release; (b) ipsilateral trunk tilt (LTT =  $-20^\circ$ ) and high shoulder abduction (SA =  $120^\circ$ ); (c) contralateral trunk tilt (LTT =  $40^\circ$ ) and low shoulder abduction (SA =  $70^\circ$ ); (d) contralateral trunk tilt (LTT =  $40^\circ$ ) and high shoulder abduction (SA =  $120^\circ$ ). Frame numbers shown at top of figures. For this participant, Frame 21 was the instant of foot contact and Frame 48 was the instant of ball release.

participant's body weight and segments lengths (Chandler, Clauser, McConville, Reynolds, & Young, 1975; Plagenhoef, Evans, & Abdelnour, 1983) (Appendix B).

For inverse dynamics, a three-link model of the throwing arm was composed of the hand with the ball, the forearm, and the upper arm before the instant of ball release. Another three-link model of the hand, forearm, and upper arm was used for after the instant of ball release. However, due to limitations in the computer resolution of the video image, the mass of the hand with the ball was assumed to be at the same position as the wrist before the instant of ball release, and the mass of the hand was assumed to be at the same position as the wrist after the instant

of ball release. The mass of the baseball was set to 0.145 kg and the moment of inertia of the ball was assumed to be negligible.

A two-way analysis of variance (ANOVA) was performed to analyze the effects of shoulder abduction angle and lateral trunk tilt angle on elbow varus torque for the simulated motions. Then, for each lateral trunk tilt angle, a one-way ANOVA investigated the effect of shoulder abduction angle on elbow varus torque. Post hoc comparisons between the condition minimizing peak elbow varus torque and the other conditions were made using the Scheffé test. *P* values were considered statistically significant if they were less than 0.05.

For the purpose of comparing the percent change of varus torque among participants, the peak elbow varus torque for each simulated motion for each participant was normalized, using the peak elbow varus torque during the actual pitching for that participant. The normalized values were used only for qualitative comparison of the percent of change of varus torque among participants.

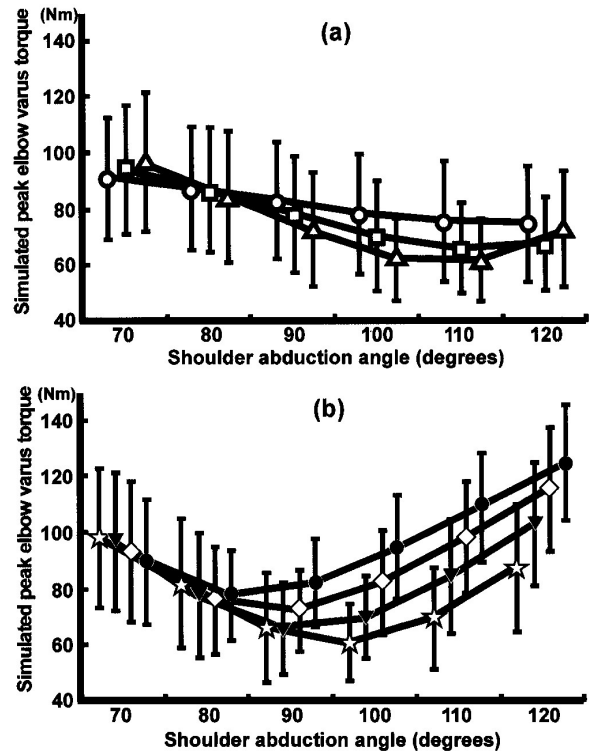
Correlation coefficients were calculated for the simple regression model, the second-order regression model, and a multiple correlation coefficient using the actual pitching data. For each coefficient, elbow varus torque was the dependent variable and shoulder abduction angle and/or lateral trunk tilt angle were the independent variables. *P* values were considered statistically significant if they were less than 0.05.

## Results

From the results of the two-way ANOVA for the simulated motions, significant interaction between shoulder abduction and lateral trunk tilt was found ( $p < 0.0001$ ). The shoulder abduction minimizing peak elbow varus torque decreased as the trunk tilted to the contralateral side.

For the ipsilateral trunk tilt conditions, the greater shoulder abduction tended to show less elbow varus torque. In the  $-20^\circ$  condition, peak elbow varus torque was minimal ( $75.1 \pm 20.1$  Nm) at  $120^\circ$  of shoulder abduction (Figure 2a). However, these changes in elbow varus torque with shoulder abduction were not statistically significant.

The  $-10^\circ$  condition and no lateral trunk tilt condition had a similar trend (Figure 2a). The peak varus torque was minimal ( $66.0 \pm 31$  Nm and  $62.1$



	70	80	90	100	110	120
(i)	-20 ○ ns	ns	ns	ns	ns	min
	-10 □ $p < .0001$	$p < .01$	ns	ns	min	ns
	0 △ $p < .0001$	$p < .001$	ns	ns	min	ns
(ii)	10 ☆ $p < .0001$	$p < .01$	ns	min	ns	$p < .0001$
	20 ▼ $p < .0001$	ns	min	ns	$p < .05$	$p < .0001$
	30 ◇ $p < .001$	ns	min	ns	$p < .0001$	$p < .0001$
	40 ● ns	min	ns	$p < .05$	$p < .0001$	$p < .0001$

**Figure 2** – Mean  $\pm$  SD of simulated peak elbow varus torque as a function of shoulder abduction. To avoid congestion of the lines, we divided 7 conditions of the lateral trunk tilt into two figures: (a) Ipsilateral conditions and no lateral condition, and (b) contralateral conditions. Bottom table shows the results of post hoc tests. Each row represents a certain lateral trunk tilt condition. In column of shoulder abduction angle condition, “min” means minimum varus torque in lateral trunk condition, and “ns” means no significant difference with minimum varus torque.

$\pm 14.4$  Nm, respectively) at  $110^\circ$  of shoulder abduction and significantly smaller than those at  $70^\circ$  of shoulder abduction and  $80^\circ$  of shoulder abduction. Significant differences were not found in any other shoulder abduction conditions.

At  $10^\circ$  of contralateral trunk tilt, peak varus torque was minimal at  $100^\circ$  of shoulder abduction ( $61.0 \pm 14.0$  Nm) (Figure 2b). The results of the post hoc test revealed significant differences with the peak varus torques in  $70^\circ$ ,  $80^\circ$ , and  $120^\circ$  of shoulder abduction conditions.

The 20° and 30° of lateral trunk tilt conditions showed a similar trend (Figure 2b). The peak elbow varus torque was minimal ( $66.7 \pm 19.0$  Nm and  $66.4 \pm 16.5$  Nm, respectively) in the 90° condition of shoulder abduction and formed a U-shape as a function of shoulder abduction angle. The peak torques at 90° were significantly smaller than those at 70°, 110°, and 120° of shoulder abduction.

For the 40° of lateral trunk tilt condition, the peak elbow varus torque was minimal ( $77.9 \pm 16.8$  Nm) in the 80° condition of shoulder abduction (Figure 2b). The torque was significantly smaller than those at 100°, 110°, and 120° of shoulder abduction.

The combination of 10° of lateral trunk tilt and 100° of shoulder abduction produced the minimum peak varus torque among all conditions in the simulated motion in the current study ( $61 \pm 14$  Nm). The greatest value of peak varus torque of the elbow ( $125 \pm 21$  Nm) was found with the combination of 120° of shoulder abduction and 40° of contralateral trunk tilt, and was more than double the smallest value of peak varus torque.

Simulations for all participants showed a similar trend in the relationship between elbow varus torque and the interaction of shoulder abduction and lateral trunk tilt. That is, peak elbow varus torque generally showed a U-shape as a function of shoulder abduction angle, and the bottom of the U-shape (the angle showing the minimum peak varus torque) shifted to a greater abduction angle as the trunk tilt angle increased ipsilaterally.

However, individual differences were found in the percent of change of elbow varus torque. For example, Figure 3 shows individual differences among three of the participants. To help show the difference between participants and the difference with peak elbow varus torque during the actual pitching for the corresponding participant, elbow varus torques of the simulated motions were represented as the value normalized by peak elbow varus torque during the actual pitching.

Based on peak elbow varus torques in the simulated motions, equivalent values of the torque (represented as a percentage of the peak torque measured for actual pitching) were connected as a contour line. Therefore the line of 100% represents all combinations of shoulder abduction and lateral trunk tilt that produce the same amount of peak elbow varus torque as produced in the actual pitching. Participant SR had 93.5° of shoulder abduction and 29.6° of contralateral trunk tilt in the actual pitching, represented as a star. SR had sparser contours than DB and MC had, meaning that SR was less sensitive to the change of either or both angles. Participant MC has the densest contours of the three examples, meaning that he was more sensitive to the change of angle(s).

For the actual pitching of the participants, the mean and standard deviation of shoulder abduction at the instant of ball release was  $93.3^\circ \pm 7.9^\circ$ , ranging from 79.8° to 109.6°. Lateral trunk tilt at the instant of ball release was  $28.9^\circ \pm 5.7^\circ$ , ranging from 18.4° to 39.3°. The mean and standard deviation of

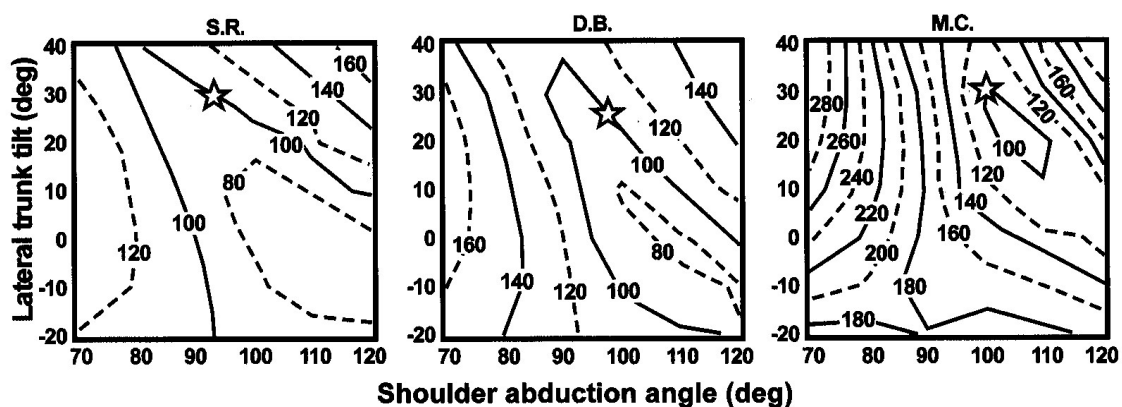


**Figure 3** – Peak elbow varus torque (normalized by actual torque) as a function of shoulder abduction and lateral trunk tilt angles for three participants (SR, DB, MC) as examples. Each contour line represents the same peak elbow varus torque normalized as a percentage of that for actual pitching. A star represents the angle combination of the shoulder abduction and lateral trunk tilt for the actual pitching.

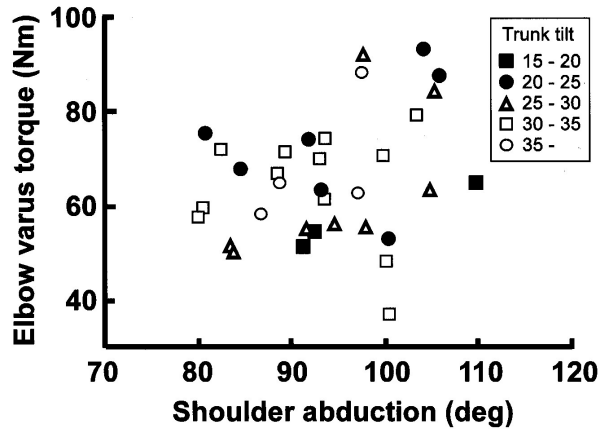


**Figure 4** – Peak elbow varus torque as a function of shoulder abduction for actual pitching, classified by lateral trunk tilt angle.

the peak elbow varus torque was  $65.0 \text{ Nm} \pm 13.0 \text{ Nm}$ , ranging from 37.1 Nm to 92.9 Nm. Figure 4 illustrates the relationships among these variables. Each symbol, such as a filled square, a filled circle, or an open triangle, shows each participant classified by lateral trunk tilt at the instant of ball release. The participants were scattered without any trends.

From the results of the regression analyses, no significant relationship was found between shoulder abduction and peak elbow varus torque ( $r = 0.216$ ,  $p = 0.227$ ). The relationship between lateral trunk tilt and peak elbow varus torque was not significant either ( $r = 0.062$ ,  $p = 0.733$ ). The correlation coefficients from the second-order regression model between the independent variables (shoulder abduction and lateral trunk tilt) and the dependent variable (peak elbow varus torque) were 0.237 ( $p = 0.421$ ) and 0.139 ( $p = 0.747$ ), respectively. A multiple correlation coefficient between peak elbow varus torque and the two independent variables was 0.231 ( $p = 0.441$ ). Thus, no significant relationships were found between dependent and independent variables.

## Discussion

The results of our simulation study clearly showed that the shoulder abduction angle affected elbow varus torque and that the peak elbow varus torque as a function of shoulder abduction generally formed a parabolic curve with minimum at a certain angle of shoulder abduction. The shoulder abduction angle minimizing the peak elbow varus torque depended

on lateral trunk tilt. McFarland (1990) recommended  $90^\circ$  of shoulder abduction for reducing torque and possible injury.

Our results of the simulation supported this recommendation, but only when the trunk bended contralaterally to  $20^\circ$  or  $30^\circ$ , typical angles of lateral trunk tilt for overhand and three-quarter-hand pitchers (Escamilla, Fleisig, Barrentine, Zheng, & Andrews, 1998; Matsuo et al., 2000). The best angle combination for minimizing peak elbow varus torque was  $100^\circ$  of shoulder abduction with  $10^\circ$  of contralateral trunk tilt. The peak elbow varus torques of these angle combinations— $90^\circ$  shoulder abduction and  $20^\circ$  contralateral trunk tilt ( $90^\circ$  ABD and  $20^\circ$  LTT),  $90^\circ$  ABD and  $30^\circ$  LTT, and  $100^\circ$  ABD and  $10^\circ$  LTT—did not significantly differ from each other. An optimal angle combination for overhand and three-quarter-hand pitchers may generally be located between these combinations.

When the trunk tilted ipsilaterally, the shoulder abduction angle minimizing the peak elbow varus torque tended to be greater than  $90^\circ$ . This did not agree with the results from a previous study (Matsuo et al., 2002), which investigated the optimal shoulder abduction angle maximizing velocity of the throwing wrist and minimizing the throwing arm kinetics. Results of their simulation, using the same simulation method as in the current study, showed that peak elbow varus torque decreased as the shoulder abduction angle decreased for underhand pitchers bending their trunk ipsilaterally.

Possible reasons for this discrepancy are kinematic differences between overhand and underhand pitching. It was reported that underhand pitchers had a more horizontally flexed arm and slower elbow extension velocity during the arm acceleration phase of pitching, as well as lower shoulder abduction and ipsilateral trunk tilt, compared to the overhand and three-quarter-hand pitchers (Matsuo et al., 2000). These differences might affect the results of the present study, which simulated overhand pitchers in an underhand position.

For all contralateral trunk tilt conditions, peak elbow varus torque showed a U-shaped curve as a function of shoulder abduction angle. For extreme conditions of shoulder abduction angle, peak varus torque showed 150% to 200% of peak varus torque in the actual pitching. Fleisig et al. (1995) reported that peak varus torque during pitching reached  $64 \pm$

12 Nm and that 54% of this torque may be generated by the ulnar collateral ligament (UCL). This was near the maximum capacity of UCL because the maximum capacity of UCL for cadavers was  $32.1 \pm 9.6$  Nm. However, this cadaveric experiment did not include the contribution of muscles around the elbow to resist valgus torque during pitching.

Buchanan, Delp, and Solbeck (1998) developed a detailed musculoskeletal model to estimate torque-generating capacity for varus and valgus torque of muscles around the elbow and found that almost all muscles could produce varus or valgus torque when the elbow is statically flexed at a right angle. Among the muscles crossing the elbow, pronator teres had the largest contribution for producing varus torque. During the late cocking phase in which peak elbow varus torque occurs, the throwing elbow was in the position of 100–110° degrees (Feltner & Dapena, 1986; Werner, Fleisig, Dillman, & Andrews, 1993) and the pronator teres showed low or moderate activity (39% to 50% manual muscle test) (DiGiovine, Jobe, Pink, & Perry, 1992; Gowan, Jobe, Tibone, Perry, & Moynes, 1987). Therefore the muscle activity of the pronator teres provides some contribution to varus torque during the late cocking phase, although it may not be sufficient. Thus it is expected that the maximum capacity of UCL during pitching may be somewhat greater than the value reported by Fleisig et al. (1995).

Nevertheless, the extreme conditions in the current simulation reached approximately 150% to 200% of peak varus torque in the actual pitching (i.e., over 100 Nm). The high torque values from these extreme angle combinations may increase the risk of injury for the elbow joint, and should probably be avoided.

The results of our regression analysis showed no significant relationships between shoulder abduction angle and elbow varus torque. It was partly consistent with the study by Sabick et al. (2004), which showed that the only variable among various kinematic variables selected into a multiple regression analysis to predict elbow varus torque was maximum shoulder external rotation. Both results from their regression analyses and our analysis did not agree with our simulation results, showing a clear effect on elbow varus torque.

Our interpretation of this discrepancy is that shoulder abduction is a potential determinant of peak elbow varus torque, but not a dominant

contributor. In the simulation study, we changed only the shoulder abduction and/or the lateral trunk tilt angle(s). The other angles in the throwing arm and the trunk movements remained the same. It is well known that some compensatory movements always occur when a certain joint moves (Saltzman & Kelso, 1987). Although the current approach assumed that compensatory movement occurred in only the nonthrowing arm, compensation may also occur in the throwing arm and the trunk movements during actual pitching. Therefore the other movements, such as shoulder external rotation shown in the study by Sabick et al. (2004), might affect elbow varus torque to a much greater extent than shoulder abduction did.

Werner et al. (2002) also suggested that elbow varus torque was predictable using peak angular velocity of shoulder horizontal adduction, maximum torque of shoulder internal rotation, elbow angle at the instant of peak varus torque, and shoulder abduction angle. These variables may have been related to varus torque in the current study as well. Among these variables in Werner et al.'s study, maximum torque of shoulder internal rotation seemed a crucial determinant. Its standardized partial regression coefficient was 14 times that for the shoulder abduction angle. Shoulder abduction could affect the varus torque only 1/27th as much as the maximum torque of shoulder internal rotation. The influence of several movements other than shoulder abduction might have masked the effect of shoulder abduction in the single regression analysis.

The other possible cause of the difference between the results from the simulation and the regression in our study was the range of shoulder abduction angle and trunk tilt angle. The ranges of actual shoulder abduction angle and trunk tilt angle among participants were smaller than simulated angles. If in reality there were participants with shoulder abduction and trunk tilt angle at both the high and low ends of our simulated angles, there might have been significant relationships between these angles and peak elbow varus torque.

As mentioned above, Werner et al. (2002) identified shoulder abduction angle at stride foot contact as one of the predictors for elbow varus torque in their multiple regression analysis. The results of their multiple regression equation suggested that the greater shoulder abduction angle

led to greater elbow varus torque and vice versa. Our results provide further insight into their results, assuming that the shoulder abduction angle did not change much from the instant of stride foot contact to the instant of ball release.

This assumption is supported by the results of several other studies (Dillman, Fleisig, & Andrews, 1993; Fleisig et al., 1996). Since shoulder abduction angle at the instant of stride foot contact, in Werner's (2002) study, was  $109^\circ \pm 33^\circ$ , their data correspond mainly to the right half of the parabolic curve in the current study, where a positive relationship between elbow varus torque and shoulder abduction was shown. It should not be applied when the abduction angle is below  $100^\circ$ . The assumption of a linear relationship in the multiple regression analysis should be applied only to a limited range of abduction angles.

Because the density of the contours indicated sensitivity of the elbow varus torque to the change of angles, a pitcher having sparser contours may have an advantage because peak elbow varus torque would not increase so much even when a pitcher changes his kinematics for some reason, such as fatigue. For example, for participant SR in Figure 3, changing his shoulder abduction from  $100^\circ$  to  $90^\circ$  did not induce any additional varus torque on his elbow. On the other hand, when the shoulder abduction angle for MC decreased from  $100^\circ$  to  $90^\circ$ , peak elbow varus torque increased by 1.8 times. Thus the current simulation approach can be used as a sensitivity analysis.

Regression analysis represents a more realistic phenomenon than the current simulations. On the other hand, the results of our simulation study reflected the direct influence of shoulder abduction on the elbow varus torque, dissociated from any other determinants. It is a merit, but also a major limitation. As mentioned above, the current approach assumed that compensatory movement occurred in only the nonthrowing arm and that angular velocities did not change. These assumptions may not be realistic but are limitations of this study, because it has not been elucidated how compensatory movements occur when a thrower tries to change his/her shoulder abduction angle for the throwing shoulder or lateral trunk tilt angle during pitching. An empirical investigation would be very challenging because it might expose participants to a risk of injury. Forward

simulation with some constraint conditions, being validated by the evidences of such compensatory movements, is needed to resolve such problems in the future.

The elbow varus torque calculated in this study may have contained some systematic errors, caused by assumption of mass location of the hand-ball segment, ignoring wrist and forearm movements, sub-optimal marker placement protocol, and nonprecise joint center estimation. These limitations resulted mainly from the wide range of motion during pitching, very fast and complicated throwing arm movement, number of cameras used, and resolution of the cameras. Although the amplitude of varus torque might be influenced by these limitations, the main patterns and trends may not have been.

## References

- Abdel-Aziz, Y.I., & Karara, H.M. (1971). Direct linear transformation from comparator coordinates into object space coordinates in close-range photogrammetry. In *Proceedings of the American Society of Photogrammetry Symposium on Close-Range Photogrammetry* (pp. 1-18). Falls Church, VA: American Society of Photogrammetry.
- Albright, J.A., Jokl, P., Shaw, R., & Albright, J.P. (1978). Clinical study of baseball pitchers: Correlation of injury to the throwing arm with method of delivery. *American Journal of Sports Medicine*, **6**, 15-21.
- Andrews, J.R., & Timmerman, L.A. (1995). Outcome of elbow surgery in professional baseball players. *American Journal of Sports Medicine*, **23**, 407-413.
- Buchanan, T.S., Delp, S.L., & Solbeck, J.A. (1998). Muscular resistance to varus and valgus loads at the elbow. *Transactions of the ASME Ser. K. Journal of Biomechanical Engineering*, **120**, 634-639.
- Chandler, R.F., Clauser, C.E., McConville, J.T., Reynolds, H.M., & Young, J.W. (1975). *Investigation of the inertial properties of the human body*. Technical Report (DOT HS-801 430). Dayton, OH: Wright-Patterson Air Force Base.
- DiGiovine, N.M., Jobe, F.W., Pink, M., & Perry, J. (1992). An electromyographic analysis of the upper extremity in pitching. *Journal of Shoulder and Elbow Surgery*, **1**, 15-25.
- Dillman, C.J., Fleisig, G.S., & Andrews, J.R. (1993). Biomechanics of pitching with emphasis upon shoulder kinematics. *Journal of Orthopaedic and Sports Physical Therapy*, **18**, 402-408.
- Escamilla, R.F., Fleisig, G.S., Barrentine, S.W., Zheng, N., & Andrews J.R. (1998). Kinematic comparisons of throwing different types of baseball pitches. *Journal of Applied Biomechanics*, **14**, 1-23.
- Feltner, M., & Dapena, J. (1986). Dynamics of the shoulder and elbow joints of the throwing arm during a baseball pitch. *International Journal of Sport Biomechanics*, **2**, 235-259.

Fleisig, G.S., Andrews, J.R., Dillman, C.J., & Escamilla, R.F. (1995). Kinetics of baseball pitching with implications about injury mechanisms. *American Journal of Sports Medicine*, **23**, 233-239.

Fleisig, G.S., Escamilla, R.F., Andrews, J.R., Matsuo, T., Satterwhite, Y., & Barrentine, S.W. (1996). Kinematic and kinetic comparison between baseball pitching and football passing. *Journal of Applied Biomechanics*, **12**, 207-224.

Gowan, I.D., Jobe, F.W., Tibone, J.E., Perry, J., & Moynes, D.R. (1987). A comparative electromyographic analysis of the shoulder during pitching. Professional versus amateur pitchers. *American Journal of Sports Medicine*, **15**, 586-590.

House, T. (1990). *The pitching edge*. Champaign, IL: Human Kinetics.

Klinge, K.E., & Kocher, M.S. (2002). Little league elbow—Valgus overload injury in the paediatric athlete. *Sports Medicine*, **32**, 1005-1015.

Matsuo, T., Matsumoto, T., Mochizuki, Y., Takada, Y., & Saito, K. (2002). Optimal shoulder abduction angles during baseball pitching from maximal wrist velocity and minimal kinetics viewpoints. *Journal of Applied Biomechanics*, **18**, 306-320.

Matsuo, T., Takada, Y., Matsumoto, T., & Saito, K. (2000). Biomechanical characteristics of sidearm and underhand baseball pitching: Comparison with those of overhand and three-quarter-hand pitching. *Japanese Journal of Biomechanics in Sports and Exercise*, **4**, 243-252.

McFarland, J. (1990). *Coaching pitchers*. Champaign, IL: Human Kinetics.

Nobuhara, K. (2003). The shoulder in sports. In K. Nobuhara (Ed.), *The shoulder: Its function and clinical aspects* (pp. 401-460). Toh Tuck Link, Singapore: World Scientific Publ.

Norwood, L.A., Del-Pizzo, W., Jobe, F.W., & Kerlan, R.K. (1978). Anterior shoulder pain in baseball pitchers. *American Journal of Sports Medicine*, **6**, 103-105.

Petty, D.H., Andrews, J.R., Fleisig, G.S., & Cain, E.L. (2004). Ulnar collateral ligament reconstruction in high school baseball players: Clinical results and injury risk factors. *American Journal of Sports Medicine*, **32**, 1158-1164.

Plagenhoef, S., Evans, F.G., & Abdelnour, T. (1983). Anatomical data for analyzing human motion. *Research Quarterly for Exercise and Sport*, **54**, 169-178.

Sabick, M.B., Torry, M.R., Lawton, R.L., & Hawkins, R.J. (2004). Valgus torque in youth baseball pitchers: A biomechanical study. *Journal of Shoulder and Elbow Surgery*, **13**, 349-355.

Saltzman, E., & Kelso, J.A. (1987). Skilled actions: A task-dynamic approach. *Psychological Review*, **94**, 84-106.

Werner, S.L., Fleisig, G.S., Dillman, C.J., & Andrews, J.R. (1993). Biomechanics of the elbow during baseball pitching. *Journal of Orthopaedic and Sports Physical Therapy*, **17**, 274-278.

Werner, S.L., Murray, T.A., Hawkins, R.J., & Thomas, J.G. (2002). Relationship between throwing mechanics and elbow valgus in professional baseball pitchers. *Journal of Shoulder and Elbow Surgery*, **11**, 151-155.

Zheng, N., Fleisig, G.S., Barrentine, S.W., & Andrew, J.R. (2004). Biomechanics of pitching. In G. Hung & J. Pallis (Eds.), *Biomedical engineering principles in sports* (pp. 209-256). New York: Kluwer Academic/ Plenum Publ.

### Appendix A. Calculation for Local Coordinates and Joint Angular Parameters

A global reference frame ( $R_g$ ) and local reference frames ( $R_p$ ,  $R_t$ , and  $R_u$ ) are shown in Figure A. Subscripts g, p, t, and u stand for global, pelvis, trunk, and upper arm, respectively. Each axis in all coordinates is a unit vector:

For the trunk local coordinate:

- $Y_t$ : mid-hips to mid-shoulders,
- $X_t$ : cross-product of  $Y_t$  and a vector from left shoulder to right shoulder,
- $Z_t$ : cross-product of  $X_t$  and  $Y_t$ .

For the pelvis coordinate:

- $Z_p$ : left hip to right hip,
- $X_p$ : cross-product of  $Y_t$  and  $Z_p$ ,
- $Y_p$ : cross-product of  $Z_p$  and  $X_p$ .

For the upper arm coordinate:

- $Z_u$ : throwing shoulder to throwing elbow,
- $X_u$ : cross-product of  $Y_t$  and  $Z_u$ ,
- $Y_u$ : cross-product of  $Z_u$  and  $X_u$ .

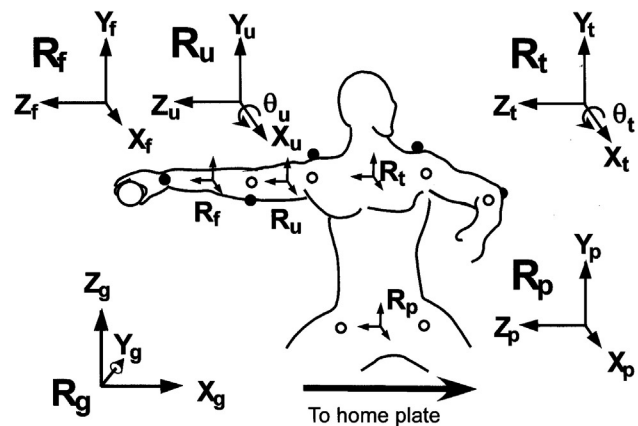


Figure A – Global reference frame ( $R_g$ ) and local reference frames ( $R_p$ ,  $R_t$ , and  $R_u$ ).

## Appendix B. Inverse Dynamic Equations of Newton-Euler Method

For inverse dynamic equations, the Newton-Euler method was used. Since the longitudinal movement of the forearm could not be measured owing to the limitation of camera resolution, its angular velocity and acceleration were ignored (Fleisig et al., 1995; 1996).

$$\begin{aligned}
 F_{f,d} &= -m_h a_h + m_h g \\
 F_{f,p} &= m_f a_f - m_f g - F_{f,d} \\
 F_{u,p} &= m_u a_u - m_u g + F_{f,p} \\
 M_{f,p,x} &= I_{f,t} \alpha_{f,x} - r_{f,d} TF_{f,d,y} - r_{f,p} TF_{f,p,y} \\
 M_{f,p,y} &= I_{f,t} \alpha_{f,y} - r_{f,d} TF_{f,d,x} - r_{f,p} TF_{f,p,x} \\
 M_{f,p,z} &= 0 \\
 M_{u,p,x} &= I_{u,t} \alpha_{u,x} - (I_{u,t} - I_{u,l}) \omega_{u,y} \omega_{u,z} + r_{u,d} TF_{f,p,y} - r_{u,p} TF_{u,p,y} - M_{f,p,x} \\
 M_{u,p,y} &= I_{u,t} \alpha_{u,y} - (I_{u,t} - I_{u,l}) \omega_{u,z} \omega_{u,x} + r_{u,d} TF_{f,p,x} - r_{u,p} TF_{u,p,x} - M_{f,p,y} \\
 M_{u,p,z} &= I_{u,t} \alpha_{u,z}
 \end{aligned}$$

where  $F$  = force,  $M$  = torque.  $TF$  represents force transformed into local reference frame;  $r$  represents distance from center of mass for each segment to either end of the segment. Subscripts  $h$ ,  $f$ , and  $u$  represent hand, forearm, and upper arm, respectively. Subscripts  $d$ ,  $p$ ,  $l$ , and  $t$  represent distal joint, proximal joint, longitudinal axis, and transverse axis, respectively. Subscripts  $x$ ,  $y$ , and  $z$  represent three orthogonal axes in a local reference frame.  $I$ ,  $\alpha$ , and  $\omega$  are the moment of inertia, the first derivative of angular velocity, and angular velocity, respectively.